MODELLING GEOTHERMAL RESERVOIRS – RECENT DEVELOPMENTS

S. P. White and W. M. Kissling
Applied Mathematics Group
Industrial Research Ltd

SUMMARY - This paper presents recent work done by Applied Mathematics group to improve our ability to model heat, mass and chemical transport in geothermal reservoirs. This work is mainly concerned with extensions to the geothermal simulator **MULKOM** written by Pruess and others at Lawrence Berkeley Laboratory. Changes in numerical algorithms used by the program have made it possible to solve moderate sized problems on Intel **386** (and up) based machines. The range of temperatures and pressures that may be modelled has been extended to **800°C** and **1000** bars.

1 Intmduction

There are three areas of where we have been working to improve our ability in geothermal modelling. These are:

1. Increase the numerical accuracy of a model. This requires more elements to be used to define a model.
2. Modelling the transport of chemicals including dissolution and precipitation.
3. Extend the range of temperatures and pressures that can be modelled.

This work extends the geothermal simulator **MULKOM** (Pruess **1983).** The motivation behind this work is twofold. Firstly, we are interested in developing a better understanding of the physical and chemical processes involved in the interaction of water with hot rocks. Secondly, by improving our modelling tools we are better able to predict the effects of exploitation of geothermal resources and thus contribute toward efficient use of the resource.

2 Mathematical Preliminaries

Before considering the new developments we briefly review the mathematical equations that describe mass, heat and chemical flow in a geothermal field and outline one numerical technique that may be used in their solution.

The conservation equations for heat, mass and a single chemical species are:

$$\begin{aligned} \frac{\partial \rho_E}{\partial t} + \nabla . j_E &= Q_E \text{ (Energy)} \\ \frac{\partial \rho_M}{\partial t} + \nabla . j_M &= Q_M \text{ (Mass)} \\ \frac{\partial \rho_s}{\partial t} + \nabla . j_s &= Q_s \text{ (Chemical)} \end{aligned} \tag{1}$$

where the density terms are given by

$$\begin{aligned} \rho_s &= \phi X \rho_b \\ \rho_M &= \phi \rho_b S + \phi \rho_v (1 - S) \\ \rho_E &= (1 - \phi)\rho_m U_m + \phi \rho_b U_b S + \phi \rho_v U_v (1 - S) \end{aligned} \tag{2}$$

and the fluxes

$$\begin{aligned} j_s &= \rho_b X q_b \\ j_M &= \rho_b q_b + \rho_v q_v \\ j_E &= \rho_b h_b q_b + \rho_v h_v q_v - K \nabla T \end{aligned} \tag{3}$$

Most of the symbols used in these equations are defined in **Table 1. Symbols** not defined there are # the porosity, K the rock matrix conductivity and source

terms Q_E, Q_M, Q_s. These equations do not apply in temperature and pressure regimes where the rock matrix properties are altered. The volume fluxes q_b and q_v are given by Darcy's equation

$$\begin{aligned} q_b &= -k\frac{k_b}{\mu_b}(\nabla P - \rho_b g) \\ q_v &= -k\frac{k_v}{\mu_v}(\nabla P - \rho_v g) \end{aligned} \tag{4}$$

These equations are solved numerically by dividing the domain of interest into a (large) number of elements, as illustrated in Figure 1. MULKOM solves for the thermodynamic state (P, T etc.) of each element and the flows of mass, energy and chemical species between them.

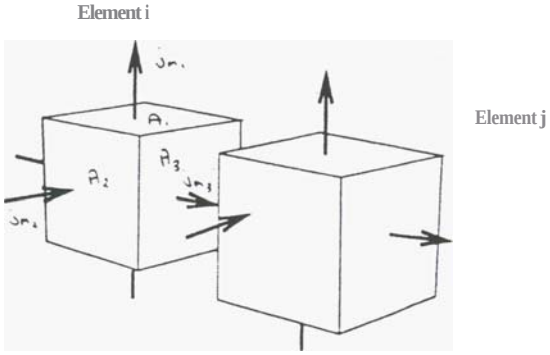

Figure 1: Typical MULKOM elements

If we assume that the elements are small enough so that fluid properties may be regarded as constant then for a typical element (i say) we can write for, example, mass conservation fiom equation 2 as:

$$f_{3i-1} = \frac{\rho^{t+\Delta t} - \rho^t}{\Delta t} + \frac{1}{V}\sum_{sides} A_i j_{m_i} - \frac{1}{2}(Q_m^{t+\Delta t} + Q_m^t) = 0 \tag{5}$$

The volume flux q_b across a side separating elements i and j are given by a discretized Darcy's law.

$$q_{b_{ij}} = -k\frac{k_b^*}{\mu_v^*}\left(\frac{P_i - P_j}{D}\right) \tag{6}$$

The quantities marked * represent some form of average of the appropriate property in elements i and j. D is the distance between element "centres".

The conservation of energy and chemical species fiom equations 2 can be discretized in a similar manner.

This process gives three nonlinear equations for each element. The unknowns in the system of equations defined by 5 are listed in Table 1.

X	(mass fraction of chemical)
ρ_b	(density of liquid)
ρ_v	(density of vapour)
S	(liquid saturation)
U_b	(internal energy of liquid)
U_v	(internal energy of vapour)
T	(temperature)
P	(pressure)

Table 1. Unknowns in equations 2.

Apart fiom X these unknowns are not independent but are related by equations defining the thermodynamic properties of the liquid and vapour. We can choose X and any other two independent combinations of the remaining variables. For example for single phase flow P and T are often chosen with P and S used for two phase flow. However, these are not the only choices, we could equally well choose P and flowing enthalpy ($H = \frac{k_b}{\mu_b}H_b + \frac{k_v}{\mu_v}H_v$) or density ($\rho = S\rho_b + (1-S)\rho_v$) and temperature as the primary variables. Whatever primary variables are chosen the numerical solution of the system of equations obtained by discretization of equations 2 for all elements proceeds in the same way.

Define a solution vector

$$x = (x_1, x_2, x_3, \cdots, x_{3N-2}, x_{3N-1}, x_{3N})^T \tag{7}$$

where x_1, x_2, x_3 are the chosen primary variables at element 1, $x_{3(j-1)+1}, x_{3(j-1)+2}, x_{3(j-1)+3}$ at element j, and so on. The conservation equations 2 for all elements can be written the form

$$F = (f_1(x_1, x_2, x_3), f2(), \cdots, f_N())^T = 0 \tag{8}$$

where f_i is defined in equation 5.

Equation 8 is solved using the Newton iteration defined by:

$$\begin{aligned} x^{i+1} &= x^i - J^{-1}(x^i)F(x^i) \\ &\text{or} \\ J(x^i)\Delta x &= -F(x^i) \end{aligned} \tag{9}$$

Here J is the Jacobian matrix of the system $J_{ij} = \frac{\partial f_i}{\partial x_j}$ and Δx is the update to the solution vector x.

For large problems by far the most time consuming part of the numerical solution of equation 8 is the calculation of Δx from equation 9.

The structure of the matrix J makes direct sparse matrix methods such as the Harwell routine MA28 unattractive for many problems. The large bandwidths that result in 3D problems, mean direct methods require prohibitive amounts of both CPU time and

memory. 2D problems (see Figure 2.) can be solved but there are attractive alternative methods available . There are a range of iterative methods that can be used to solve equations such as 9, and this is an area of active research for numerical analysts. Some examples of more or less recently developed methods are CGS (Conjugat Gradient Squared), Bi-Cg (BiConjugat Gradient), GMRES and BiCGSTAB a variant of BiCG.

We have implemented a pre-conditional version of BiCGSTAB (Van der Vorst 1991) and this has worked well in all our tests. The choice of pre-conditioner is critical to the success of this approach. To improve the speed of solution of equation 9 we modify the problem using a pre-conditioning matrix $K = K_1 K_2$ to be

$$\tilde{J}\Delta\tilde{x} = \tilde{R}$$

where

$$\begin{aligned} J &= K_1 \tilde{J} K_2 \\ x &= K_2 \Delta\tilde{x} \\ R &= K_1 \tilde{R} \end{aligned} \qquad (10)$$

K is chosen so that the iterative solution of equation 10 converges more quickly than the iterative solution of equation 9. TWO forms of K have proved satisfactory. In both cases K_1 and K_2 are an approximate LU factorization of J. The first approximation (which minimises storage) forces K to have the same sparsity pattern as J.

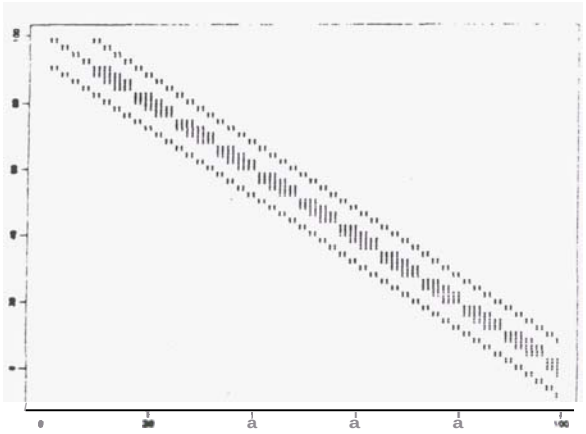

Figure 2: Example of sparse Jacobian structure

In the second method, each row of the LU factorization is calculated but the number of elements retained in that row of K is determined by two rules:

1. No more than a predetermined number of elements in a row.
2. Discard any elements that are too small.

Method 2 with a fill factor of 2 (twice as many elements in K as in J) seems to be the most effective. The disadvantage of the second method is it uses almost double the memory of the first method.

Using these techniques has greatly extended the size and geometry of problems that can be solved. For three dimensional problems the speed improvement over direct methods is a factor of at least 25. As an example of the speed up achieved a model of the Kakkonda field with over 3000 elements takes about 4 hours to simulate 15 years production from the field. Previously, if it was attempted at all, this would have taken over a week.

3 High Temperatures and Pressures

The thermodynamic routines normally used in MULKOM cover the temperature range $1 < T < 350°C$ and $1 < P < 1000$ bars. As deeper geothermal reservoirs are beginning to be exploited this temperature range is too restrictive. Temperatures of $370°C$ have been measured in existing fields and this is expected to increase as deeper wells are drilled. Fumerol temperatures in excess of $600°C$ have been measured at White Island (Giggenbach 1989). To better model these very hot areas near the region of interaction between magma and groundwater requires an extension to the thermodynamic routines used by MULKOM.

Extending the temperature and pressure range introduces two problems.

1. Above the critical temperature ($374.15°C$) water exists only in a single phase and this introduces problems in keeping track of the saturation of elements during computation.
2. At higher temperatures the thermodynamic properties are defined in terms of temperature and density not temperature and pressure as required by MULKOM.

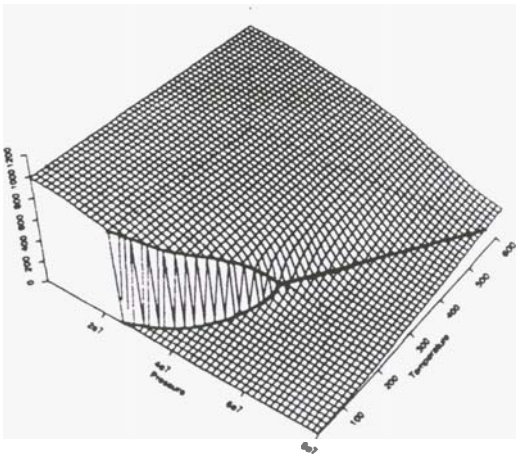

Figure 3: Water Density

Figure 3 shows the density surface for water in P,T

space. As can be seen from this plot the properties of vapour and liquid approach each other until at the critical point they become equal. Other thermodynamic properties show similar behaviour. Above the critical temperature saturation has no meaning and we can assign any value we like to it without changing any of the terms in the conservation equations 2. To exploit the existing structure of MULKOM, it is however useful to extend the "saturation" line past the critical point. This pseudo saturation line is a straight line in P,T space passing through the critical point (374.15°C, 221.2 bars) and through (800°C, 1000 bars). For a given temperature any points that have a pressure greater than the saturation pressure at that temperature are regarded as having a liquid saturation of 1. Similarly any points with pressure less than the saturation pressure are regarded as having a liquid saturation of 0.

4 Solution of Equations at High Temperatures

Normally MULKOM uses an approximation to the thermodynamic properties of water taken from the UK Steam Tables, Arnold (1970).

These steam tables divide P,T space into the regions shown in Figure 4 and use a different approximation over each region. In regions 1 and 2 properties are given as functions of P and T. In the other regions properties are functions of ρ and T.

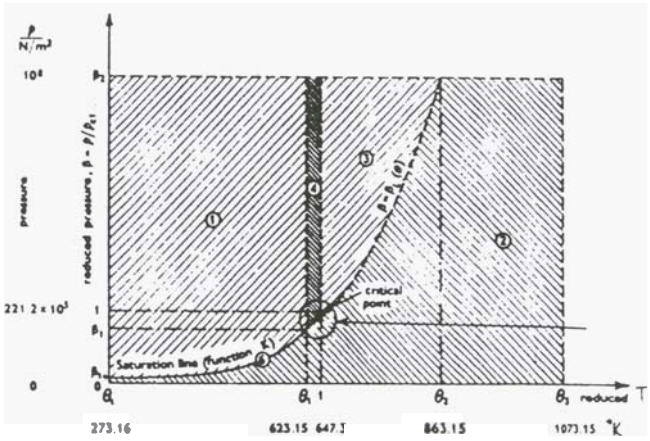

Figure 4: UK Steam Tables 1970 Formulation

This formulation can be used with P,T and X as primary variables by solving the non linear equation $P = P(\rho, T)$ in the regions above 350°C.

An alternative approximation is provided by Saul and Wagner (Saul 1989). They provide an approximation to the Helmholtz function for water in terms of ρ and T over the range $0 < T < 1000°C$ and $1 < P < 25{,}000$ bar. All the thermodynamic properties of interest can be derived from the Helmholtz function by differentiation. In order to use this approximation it is easiest to solve equation 5 using ρ and T as the primary variables. This has proved moderately successful although is slower than using P and T as primary variables below 350°C.

6 Examples

We present three examples of the use of these new MULKOM features.

1. Injection of high chloride water near a fracture and the modelling of chloride concentration as a precursor to thermal breakthrough.
2. Heating and cooling of a single element to illustrate the use of the pseudo saturation line.
3. A very approximate model of a volcanic island.

6 Injection near a fracture

The grid used for this problem is shown in Figure 5. A shallow (150 meters) well is being used to inject high chloride water at 110°C. Two deep production wells are producing from near the fracture. We were interested in investigating increased thermal rundown of the producing wells caused by the high permeability flowpath between production and injection wells provided by the fracture. This model also provides information on the use of chloride concentration as a precursor to thermal rundown.

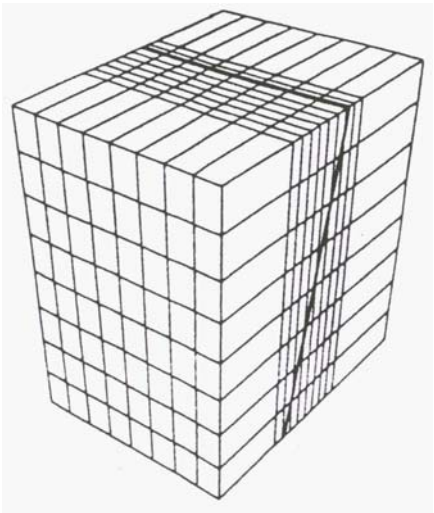

Figure 5: Grid for Fracture Model

Figures 6 (after 7.5 years) and Figure 7 (after 15 years) show the expansion of the 750 mg/kg iso-surface. This clearly shows the path of injected water down the fracture and out towards the production wells.

Figure 6: Chloride iso-surface after 7.5 years

Figure 7: Chloride iso-surface after 15 years

Figure 8 shows the calculated production temperatures and chloride concentrations at one of the production wells.

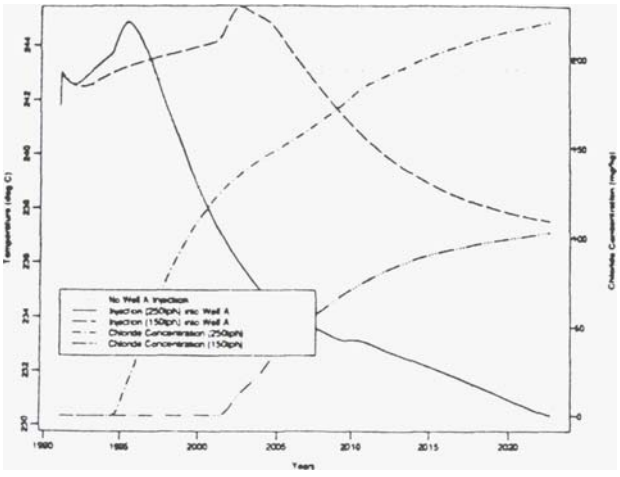

Figure 8: Production Temperatures

7 Heating and cooling an element

In this example heat and mass were added to or extracted from an element to illustrate the high temperature - pressure capability of MULKOM. In particular it shows how it is possible to move from liquid to vapour phase via the supercritical region without a discontinous change in thermodynamic properties. Initially the element contains liquid water at 20 bars and 200°C. First, there is an isothermal increase in the pressure to 600 bars. Then heat is added to increase the temperature to 600°C. As the temperature reaches the saturation temperature the water begins boiling and the temperature and pressure of the two phase mixture follow the saturation line to the critical point.

As the temperature and pressure continue to increase temperature and pressure leave the extended saturation line and we consider the fluid to be liquid water. The fluid then crosses the extended saturation line and is then considered to be vapour. Note that as there is no jump in thermodynamic properties in this crossing there is no following of the saturation line.

The remainder of the diagram shows the lowering of pressure by extracting mass and finally the lowering of temperature to bring the fluid back to the (real) saturation line fiom the vapour side. This cycle is shown in Figure 9.

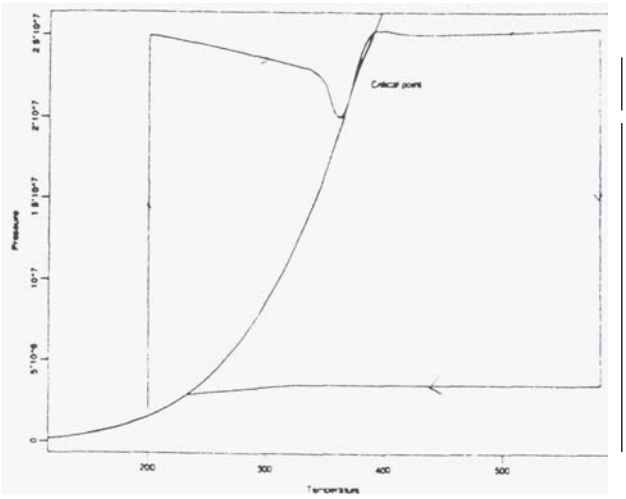

Figure 9: Heating and Cooling an Element

8 Volcanic Island

This example demonstrates the use of the extended thermodynamic routines to calculate the pressure and temperature within a cylinder of rock which is immersed in an infinite cold sea and heated from below by a 700°C hot plate. Figure 10 shows the geometry of the island and Figures 11 and 12 show the (approximately steady state) temperature and saturation profiles.

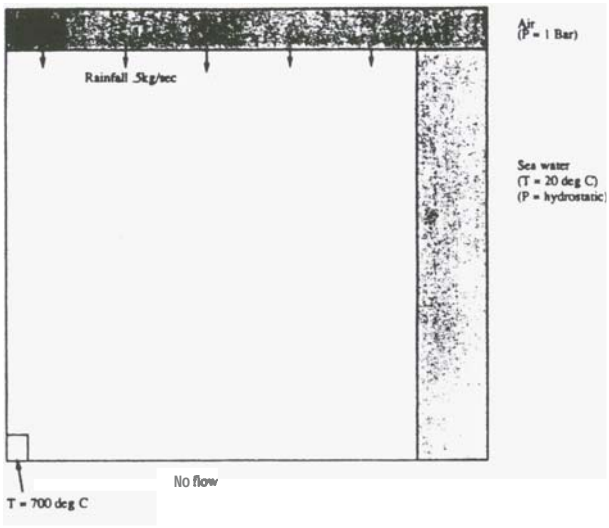

Figure 10: Volcanic Island Geometry

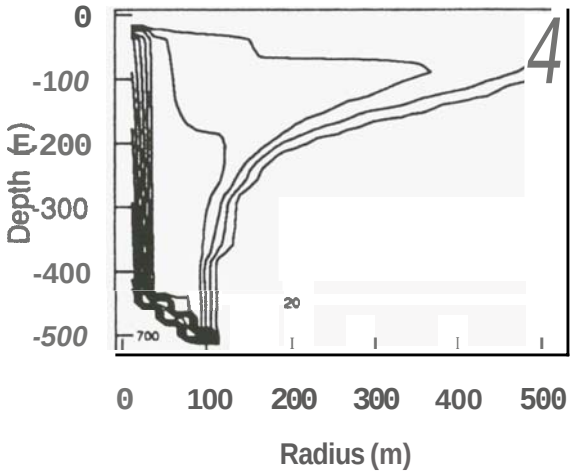

Figure 11: Temperature Contours for Volcanic Island

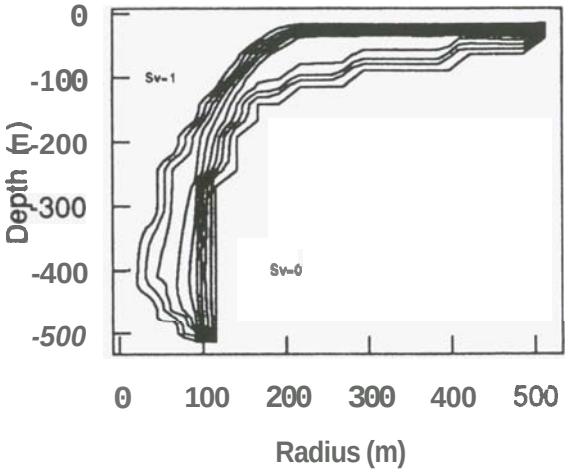

Figure 12: Saturation Contours for Volcanic Island

References

Pruess, K., 1982 ,Development of the General Purpose Simulator MULKOM, Report LBL-15500, Lawrence Berkeley Laboratory.

Arnold (Publisher), 1970 UK Steam Tables in SI Units 1970.

Saul A. and Wagner W., 1989, A Fundamental Equation for Water Covering the Range from the Melting Line to 1273K at Pressures up to 25000 MPa *J.Phys.Chem.Ref.Data*, 18 4.

Van der Vorst, H., 1991, Personal Communication.